Thrust Measurements on the T6 Hollow Cathode Thruster Using Direct Thrust Balances

IEPC-2013-129

Presented at the 33rd International Electric Propulsion Conference,
The George Washington University • Washington, D.C. • USA
October 6 – 10, 2013

D. Frollani[1]
University of Southampton, Southampton, SO17 1BJ, UK

M. Coletti[2]
Mars Space Ltd, Southampton, SO14 5FE, UK

and

S. B. Gabriel[3]
University of Southampton, Southampton, SO17 1BJ, UK

Hollow Cathodes have good flight heritage being used in GIEs and HETs since late '60s. The possibility of using them as standalone thruster (Hollow Cathode Thrusters, HCTs) has been investigated at the University of Southampton for the last ten years. In order to use HCTs to replace chemical thrusters on commercial communication satellites with HCTs to perform EWSK and wheel offloading performance requirements in terms of thrust (>0.6 mN) and specific impulse (>300 s) were obtained. In this paper the results obtained from the test of an optimized HCT based on a QinetiQ T6 neutralizer are presented. The T6 HCT was tested at UoS and AER with two different direct thrust balances in cold gas and discharge mode at 10, 15, 20 and 24 A. The thrust was measured in the discharge mode also with an applied magnetic field. The thruster was found to fulfill the requirements showing thrust up to 2.6 mN with an Isp of 260s and a maximum specific impulse of 323 s with a thrust of 1.5 mN.

Nomenclature

NSSK	=	North/South Station Keeping
EP	=	Electric Propulsion
CP	=	Chemical Propulsion
EWSK	=	East/West Station Keeping
UoS	=	University of Southampton
QQ	=	QinetiQ
AER	=	Aerospazio Tecnologie srl
MS	=	Mars Space Ltd
HC	=	Hollow Cathode
HCT	=	Hollow Cathode Thruster
GIE	=	Gridded Ion Engine
HET	=	Hall Effect Thruster

[1] PhD Researcher funded by Mars Space Ltd, Electronics and Computer Science, daniele.frollani@mars-space.co.uk
[2] Director, michele.coletti@mars-space.co.uk
[3] Professor, Electronics and Computer Science, sbg2@soton.ac.uk

ESA = European Space Agency
PSCU = Power Supplies and Control Unit
Xe = Xenon
T = Thrust
Isp = Specific Impulse
V = Discharge Voltage
Δx = Displacement of the mirror of the thrust balance
ω = Frequency of the thrust balance assembly
ϑ = Angular displacement of the thrust balance
L_r = Distance between pivot and mirror
L_{cm} = Distance between pivot and center of mass
L_t = Distance between pivot and point of thrust application
L_m = Distance between pivot and weight applied for calibration
M = Mass of the thrust balance assembly
m = Mass of the weight applied for calibration
k = Torsional spring constant of the balance assembly
K = Torsional spring constant of the balance assembly including effect of gravity
J_{bal} = Moment of inertia of the balance assembly
J_m = Moment of inertia of the weight applied for calibration
D_{int} = Internal diameter
D_{est} = External diameter
C_σ = Level of confidence of the error budget

I. Introduction

AT present, the trend in communication satellites is to perform North/South station keeping (NSSK) using electric propulsion (EP). Cold gas systems or chemical propulsion (CP) in general are instead used to perform fast attitude dynamics of a safe mode, additional wheel momentum management and dedicated East/West station keeping (EWSK) control. The benefit of EP is reduced if implemented in CP system due to the added mass of tanks, piping and propellant, power supplies and control units (PSCUs) and to the complexity of the system. The integration of the EP system performing EWSK would bring significant advantages if a single propulsion system would be used. If an EP system would replace the CP system to perform the listed maneuvers, a single propellant would be required, and there would be further benefits in mass reduction by eliminating additional tanks and PSCUs, as well as improvements in specific impulse if compared with the CP system.

In this context the use of Hollow Cathodes (HCs) as standalone thrusters (Hollow Cathode Thrusters, HCTs) would be beneficial. Hollow cathodes have been playing a key role in the field of electric propulsion since the '60s. They have been used in both Gridded Ion Engines (GIEs) and Hall Effect Thrusters (HETs) to provide discharge current and neutralization, and therefore have good flight heritage.

A set of requirements have been derived by QinetiQ taking in consideration communication geostationary satellites such as SmallGEO, EUROSTAR3000 and FS1330E, and considering that the use of HCTs must provide mass saving in comparison to the chemical thrusters now in use on these type of satellites.

System mass	< 11 kg
Power	< 500 W
Discharge mode, Isp	> 300 s
Discharge mode, T	> 0.6 mN
Cold gas mode, T	> 25 mN

Table 1. HCT Requirements

The possibility of using these devices as standalone thrusters has been investigated at the University of Southampton (UoS) by Gessini[1] and Grubisic[2], who measured the performances of QinetiQ T5 and T6 HCs for various discharge currents, mass flow rates and anode geometries[3,4,5,6] with indirect thrust balances. However such thrust measurements might not be completely reliable if a correction factor accounting for the effect of the collisions

between the propellant particles and the target of the balance is not considered [5]. If such a factor is not taken into account, thrust measurements taken with an indirect thrust balances can be overestimated up to 100%.

In this paper the results obtained from direct thrust measurements on an optimized QinetiQ T6 HCTs in cold gas and discharge mode will be shown. The experiments were carried out using two different direct thrust balances: one designed, manufactured and tested at the University of Southampton and one at Aerospazio Tecnologie srl, in Italy.

After the measurements will be presented the cathode performances will be discussed and compared to the mission requirements.

II. Hollow Cathode Thrusters

In Figure 1 the general configuration of a HCT is shown. A hollow cathode thruster is geometrically very similar to a conventional hollow cathode. The only differences can be found in the fact that the keeper electrode is replaced by and anode/nozzle and that an insulating material can be placed between the cathode orifice and the anode/nozzle to give continuity to the diverging shape optimizing the gasdynamic contribution of thrust.

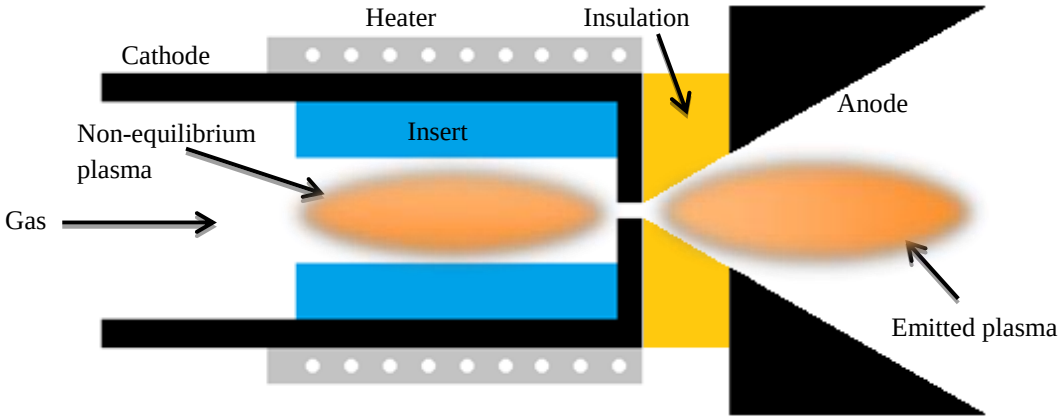

Figure 1. General HCT configuration

In this paper the thrust measurements collected with two different direct thrust balances on an optimized version of the standard QinetiQ T6 neutralizer cathode will be shown. In particular with the aid of an HCT theoretical model already developed by the University of Southampton and Mars Space Ltd [7]the length and diameter of the orifice were modified with respect to the standard T6 neutralizer design and the shape and dimensions of the anode were selected with the aim of achieving the requirements shown in Table 1. The dimensions of the HCTs tested are reported in Table 2.

Parameter	T6 HCT
Orifice length	2.5 mm (40% chamfered)
Orifice chamfering angle	45°
Orifice diameter	0.4 mm

Table 2. HCT dimensions

The T6 HCT has also been equipped with a coil wrapped around the anode/nozzle to generate a magnetic field to study its effect on the HCT performance. The coil is able to produce a maximum axial magnetic field of about 100G at 2A of coil current.

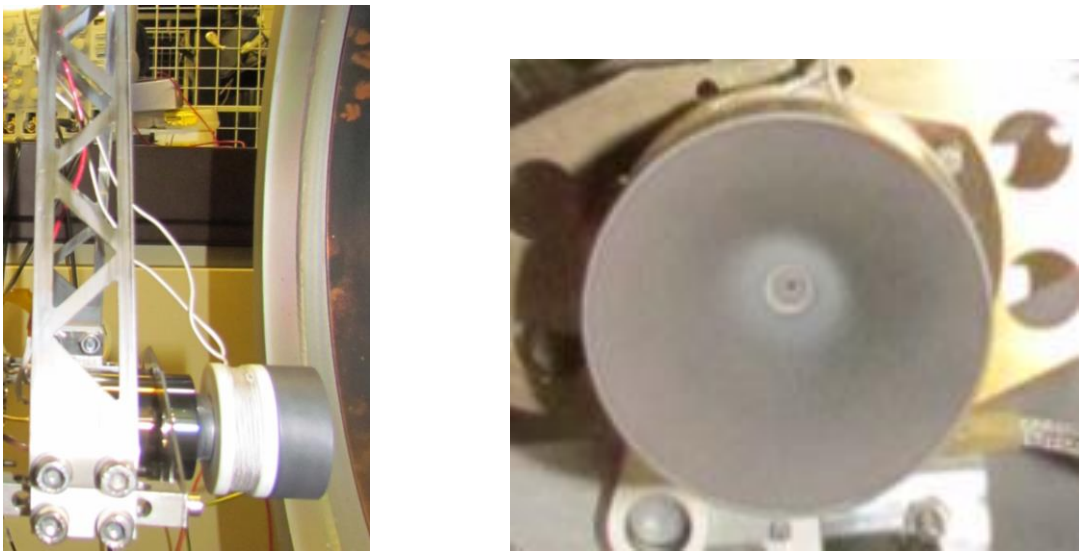

Figure 2. The optimized T6 HCT

III. UoS test setup

The tests at the UoS were performed in a vacuum chamber which was previously used to characterize the hollow cathode of the UK-25 ion engine[8] and was also used for all the previous experimental work on HCT done at the UoS[1, 2]. The vacuum system consists of a stainless steel chamber 500 mm in diameter and 500 mm long with both ISO and CF flanges. The pumping system is composed of a water-cooled turbo molecular pump Pfeiffer Balzers TPH 520KTG 500 l/s, a control unit made of a Balzers TCP 380 drive unit and a Balzers TCS 303 controller and a rotary vane pump Pfeiffer Balzers DUO 016B used as backing pump.

The vacuum pressure is monitored via a Balzers TGP 300 pressure gauge package consisting in a pirani gauge ($1000 – 5.4*10^{-4}$ mbar) and a cold cathode gauge ($5*10^{-3} – 1*10^{-9}$ mbar).

A. The thrust balance at the UoS

The thrust balance developed at UoS is a direct hanging balance; when a thrust is applied the balance moves to a displaced equilibrium position so that the torque generated by the thrust is balanced by the gravity and by the torsional spring constant of the pivot used to hang the balance harm. When the thrust is removed the balance will go back to its zero position and from the displacement the thrust can be derived.

The balance consists of a swinging arm fixed to a support structure. The displacement is measured using EUCLID[9], an optical sensor placed on a tower where two micrometer screws and a tilt stage can be used for sensor alignment. The sensor needs to be aligned to a mirror connected to the swinging arm.

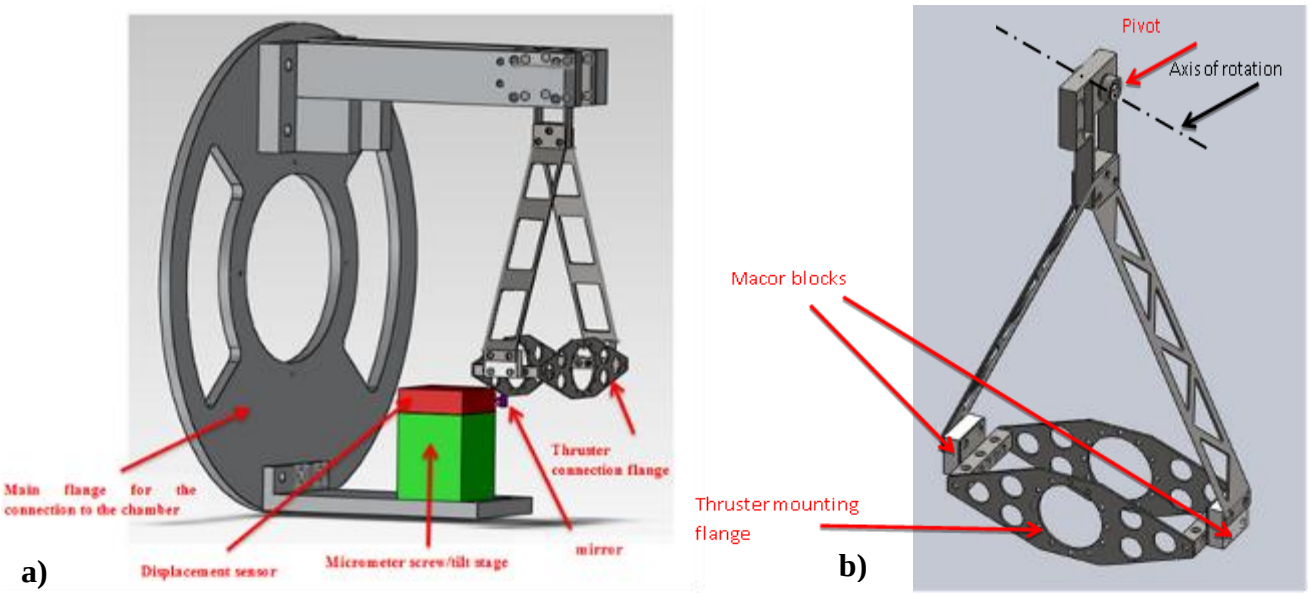

Figure 3. Complete thrust balance assembly schematic

The thrust stand, shown in Figure 3, consists of a vertical pendulum arrangement made of stainless steel with the thruster mounted on the bottom part using one mounting flange. At the other end one stainless steel pivot (*Riverhawk*[10] part number 6020-800) is mounted: this allows the arm to have only one degree of freedom. The thruster flange is thermally isolated from the rest of the balance via two *Macor* blocks to minimize heat conduction from the thruster. Nevertheless metal screws assure electrical connection between the pivot and the balance. The thrust balance is electrically grounded by its mechanical connection to the vacuum chamber.

The propellant feed line and all the electrical cables needed to operate the HCT are fixed to the pivot clamps to constrain their movement relative to the balance and reduce their torque on the balance arm as shown in Figure 4.

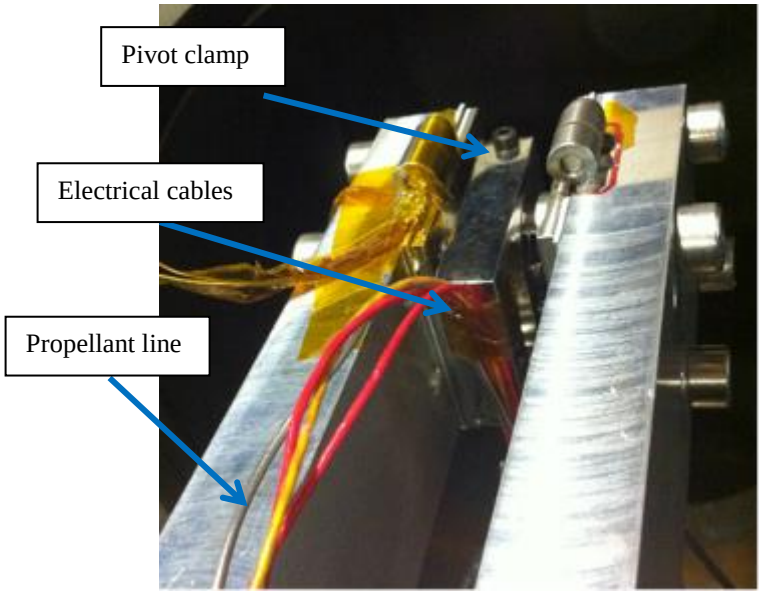

Figure 4. Top view of the thrust balance. Connection of the cables and pipe

B. The thrust balance working principle

The thrust balance is schematically shown in Figure 5, where ϑ and Δx are respectively the angular and linear arm displacement, L_r is the distance between the axis of rotation and the mirror (i.e. the displacement sensor output), L_{cm} is the distance between the axis of rotation and the center of mass and L_t is the distance between the axis of rotation and the thrust delivered by the HCT and M the mass of the balance. It is assumed that the thrust vector is parallel with the thruster symmetrical axis and applied to its center of mass. Under this assumption, L_t represents also the distance between the axis of rotation and the center of mass of the tested thruster.

Writing a torque balance around the pivot one can easily derive that the thrust can be express as

$$\textbf{(1)} \qquad T = \left(L_{cm} Mg \frac{\Delta x}{L_r} + k \frac{\Delta x}{L_r} \right) \Big/ L_t$$

as long as the displacement Δx is small enough so that $\sin(\vartheta) = \vartheta$. In equation (1) k is the torsional spring constant of the assembly formed by the pivot, the cables and propellant pipe.

Writing the differential equation that describes the dynamic response of the balance[11] it can be demonstrated that the balance natural angular frequency is:

$$\textbf{(2)} \qquad \omega = \sqrt{\frac{k + ML_{cm} g}{J_{bal}}} = \sqrt{\frac{K}{J_{bal}}}$$

where J_{bal} is the total moment of inertia of the balance assembly (including the thruster, cables and propellant lines) with respect to the axis of rotation and $K = k + ML_{cm} g_0$ is the total torsional spring constant including cables, pipes, pivot and gravity effects. Combining equation (1) and equation (2) one can obtain:

$$\textbf{(3)} \qquad T = \frac{\omega^2 J_{bal} \Delta x}{L_t L_r}$$

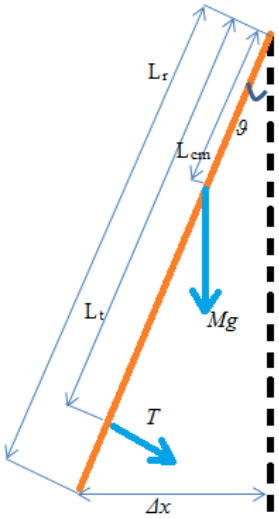

Figure 5. Thrust balance, schematics.

Equation (3) will be used to calculate the thrust since Δx and ω are obtained from the displacement sensor trace, L_t and L_r are known and J_{bal} can be measured at the beginning of the test campaign. It must be noted that the changes in the balance torsional spring constant due to thermal drifts are automatically taken into account in Eq. (3) since the thermal drifts will not significantly alter the moment of inertia or L_t and L_r and considering that the value of ω (that instead will change due to thermal effects) can be obtained from the displacement sensor signal.

The moment of inertia J_{bal} can be instead obtained with a dynamic calibration of the balance, which consists in attaching different weights to the balance and obtaining the relative angular frequency from the sensor trace. Four different weights were attached and the data were linearly fitted to obtain the balance assembly total moment of inertia as shown in Figure 6 and Table 3.

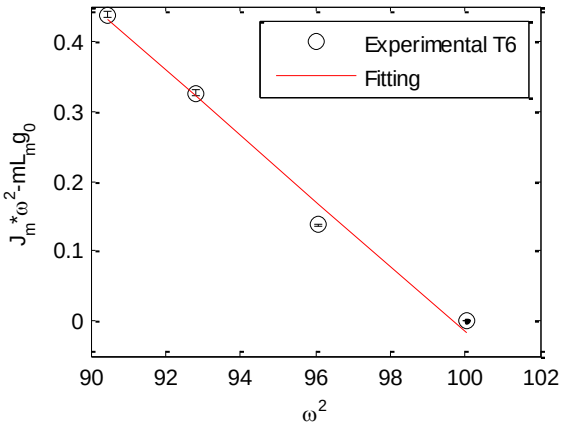

Figure 6. Dynamic Calibration for the calculation of the moment of inertia for the T6 balance assembly

	J_{bal}, kg m^2	δJ_{bal}, kg m^2
T6 HCT	0.046613	0.003714

Table 3. Moment of inertia and uncertainty at UoS

The experimental mean value of the thrust is obtained using equation (3) and its uncertainty can be expressed as:

$$\delta T = T\sqrt{\left(\frac{\delta \Delta x}{\Delta x}\right)^2 + \left(\frac{\delta L_t}{L_t}\right)^2 + \left(\frac{\delta L_r}{L_r}\right)^2 + \left(\frac{\delta J_{bal}}{J_{bal}}\right)^2 + 2\left(\frac{\delta \omega}{\omega}\right)^2} \quad \textbf{(4)}$$

Equation (6) is derived from equation (3) as all the terms can be independently measured and their errors are not correlated[12]. For what concerns L_t and L_r, they were measured with a caliper with relative uncertainties of respectively ±1.85% and ±1.45%. The uncertainty $\delta\omega$ in the measurement of ω, according to the Fast Fourier Transform algorithm, is given by:

$$\delta \omega = \frac{2\pi f_s}{2}\frac{1}{P/2+1} \quad \textbf{(5)}$$

where *fs* is the signal sampling frequency and *P* is the power of 2 closest to the number of acquired samples[13]. Since an oscilloscope with a sampling frequency of 25 kHz was used to acquire the sensor trace for a time of at least 1 minute, more than 2 million samples are acquired ($P = 2^{21}$ = 2,097,152). Thus the uncertainty in ω measurement is << 1 % and can be considered negligible. The error on the displacement is mainly due to the balance oscillations around its equilibrium position, these oscillations are dependent on the thrust level at which the thruster is run and are generally <3 %. The error on J_{bal} is reported in Table 3 and it is the biggest source of error in the measurements. Considering all what has been reported above a preliminary balance error budget is reported below:

Quantity	Error
L_t	±1.85%
L_r	±1.45%
J_{bal}	±7.9%
ω	<<1%
Δx	Measurement dependent - ~ 3%
Thrust	~ 8.7%

Table 4. Error budget

IV. AER test setup

The test was performed in the Aerospazio MVTF-1 facility, a vacuum chamber 3 meters long and 1.3 meters in diameter. The pumping system is composed of a turbo-molecular pump 700 l/s backed by a dry rotary pump, a cryopump 1500 l/s and a cold head rated for Xe pumping. The vacuum pressure is monitored via a Vacuum Gauge Leybold Ionivac ITR-90 ($1*10^{-2}$ – $1*10^{-8}$ mbar), placed on top of the chamber, approximately 40cm downstream the exhaust plane of the thruster.

The thruster was fed with and Xenon grade 4.9 using Digital Mass Flow Controllers and Meters and passed through an oxygen filter cartridge in order to trap the impurities.

The thrust balance at Aerospazio consists of a parallelogram composed of two plates (an upper one, movable, and a lower one, fixed) connected together by means of four bars and the corresponding hinges and works on the principle of the null reading. Its resolution has already been characterized experimentally as <30 μN[7].

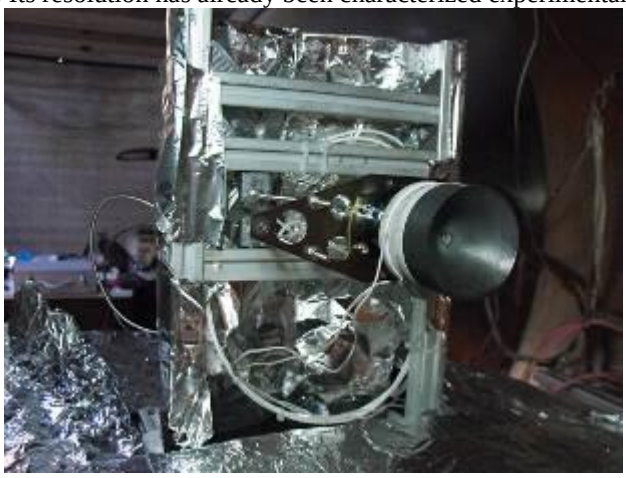

Figure 7. T6 HCTs mounted on the thrust balance at AER

V. Experimental results

Thrust measurements have been obtained with the T6 HCT using two different direct thrust balances. The T6 HCT has been characterized in both the cold gas and discharge mode without applied magnetic field, at 10, 15, 20 and 24 A of discharge current, at the UoS and with applied magnetic field at 10, 15 and 20 A of discharge current; at AER it was tested in the discharge mode without and with applied magnetic field at 10 and 15 A of discharge current. In all the experiments the value of the magnetic field used was chosen to be 86 G.

A. V-I characteristics

The V-I curves are reported below for the T6 HCT. At 5A and 10A of discharge current, the T6 HCT discharge voltage is in the range 13-29V for mass flow rates in the range 1-10 sccm of Xenon. As expected when the magnetic field is applied the discharge voltage is increased.

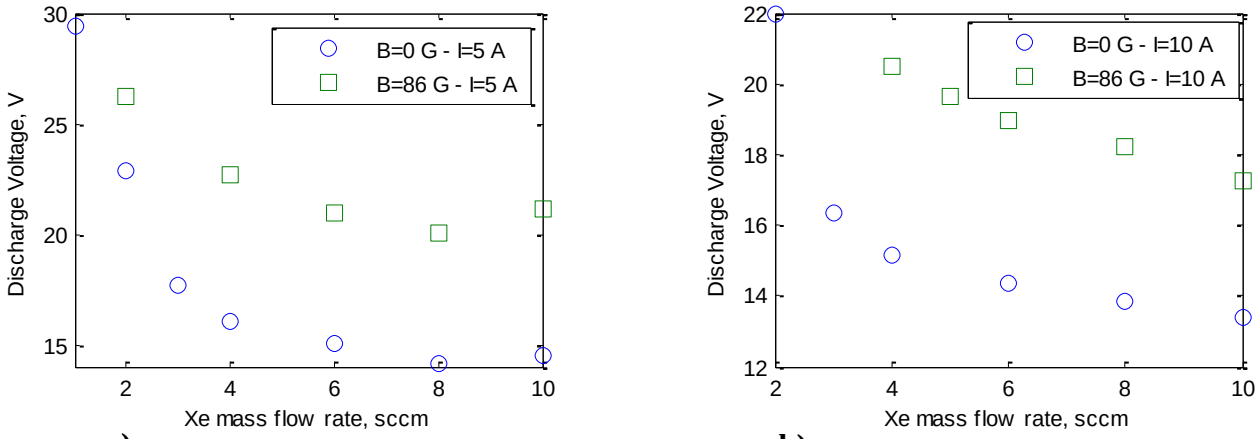

a) **b)**

Figure 8. V-I curves for the optimized T6 HCT without magnetic field and with 86G for a)5A and b)10A

Figure 9 and Figure 10 show the T6 HCT firing on the UoS thrust balance at 5 and 10 A with and without the magnetic field. It can be noticed how the application of magnetic field produces a denser plume on the thruster axis.

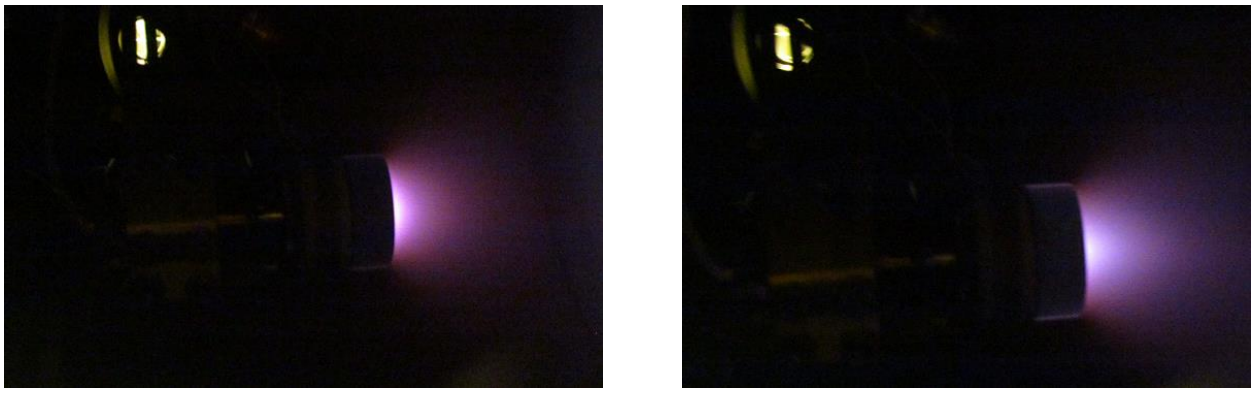

a) **b)**

Figure 9. Discharge at 5A and 6 sccm a) without the magnetic field and b) with 86G

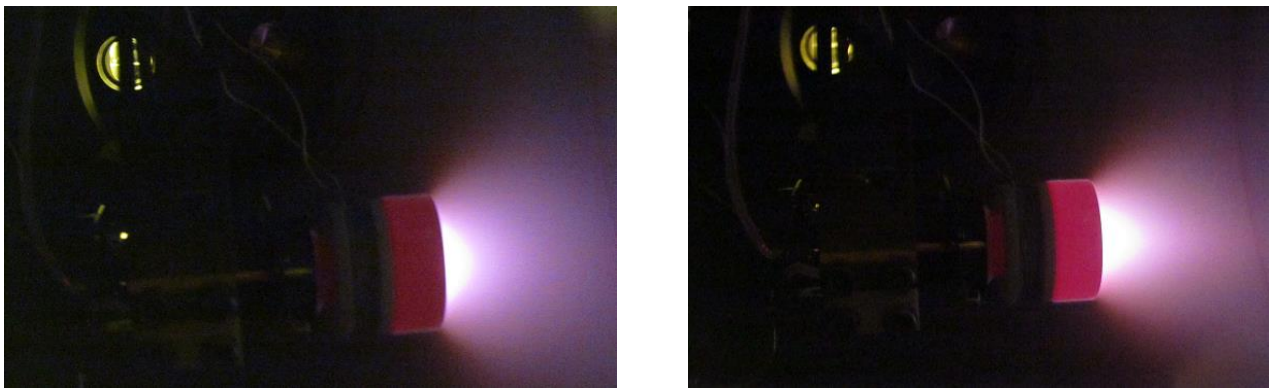

a) **b)**

Figure 10. Discharge at 10A and 5 sccm a) without the magnetic field and b) with 86G

Figure 11-a) shows the discharge voltage at 15A whereas Figure 11-b) at 20A of discharge current. Again the magnetic field increases the discharge voltage, and this increase is higher for bigger mass flow rates.

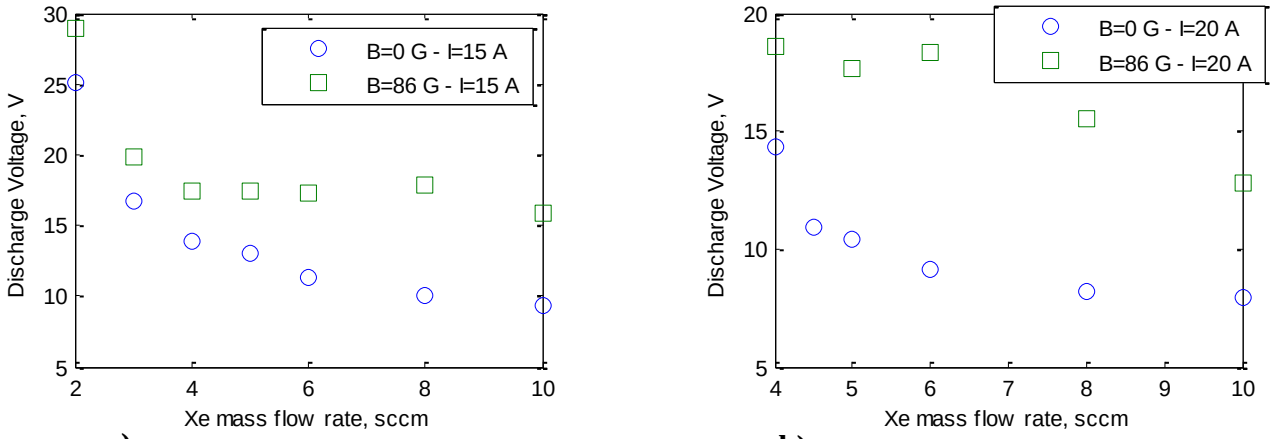

a) **b)**

Figure 11. V-I curves for the optimized T6 HCT without magnetic field and with 86G for a)15A and b)20A

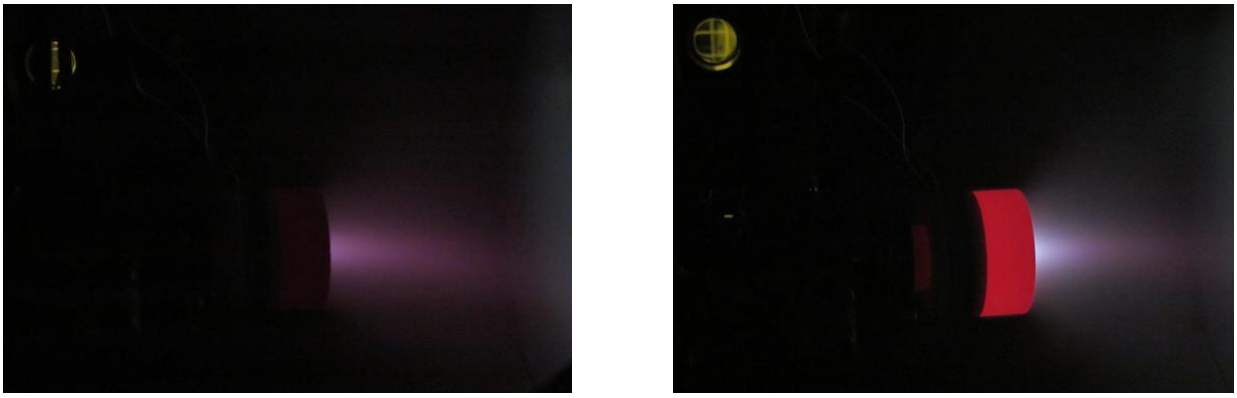

a) **b)**

Figure 12. Discharge at 15A and 6 sccm a) without the magnetic field and b) with 86G

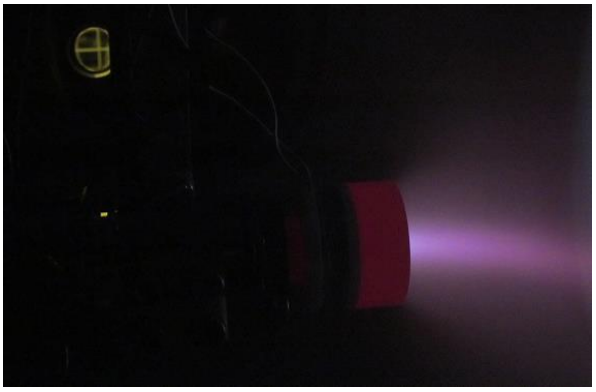

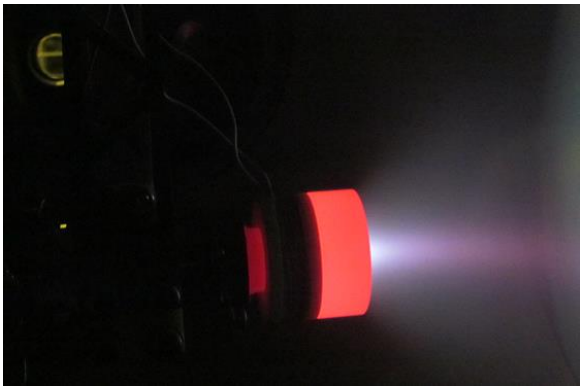

a) **b)**

Figure 13. Discharge at 20A and 6 sccm a) without the magnetic field and b) with 86G

At 24A of discharge current the increase of the discharge voltage due to the magnetic field is lower for bigger mass flow rates.

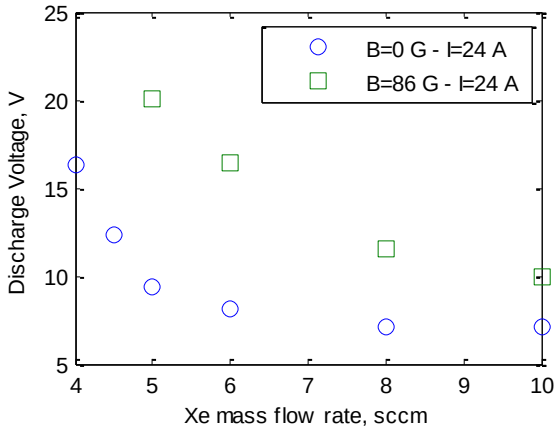

Figure 14. V-I curves for the optimized T6 HCT without magnetic field and with 86G for 24A

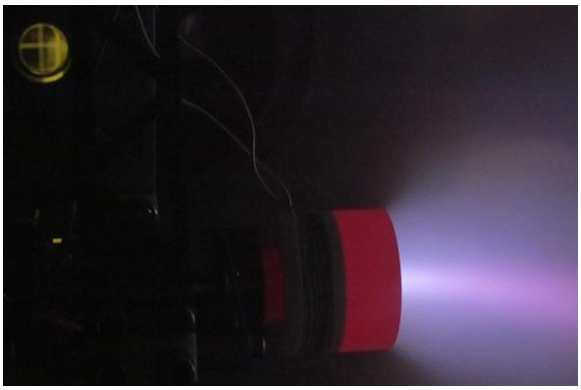

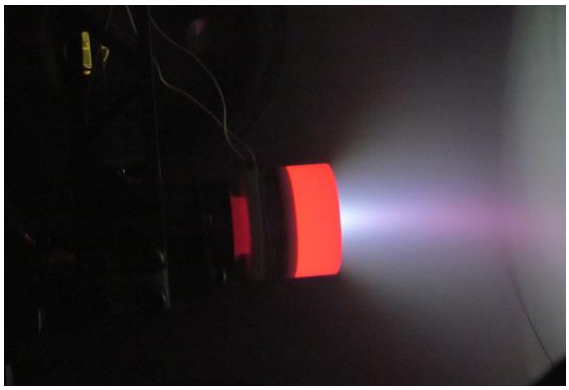

a) **b)**

Figure 15. Discharge at 24A and 6 sccm a) without the magnetic field and b) with 86G

In the discharge voltages for the T6 HCT at 10, 15, 20 and 24 A are reported whereas in Figure 16-b the data with applied magnetic field are summed up.

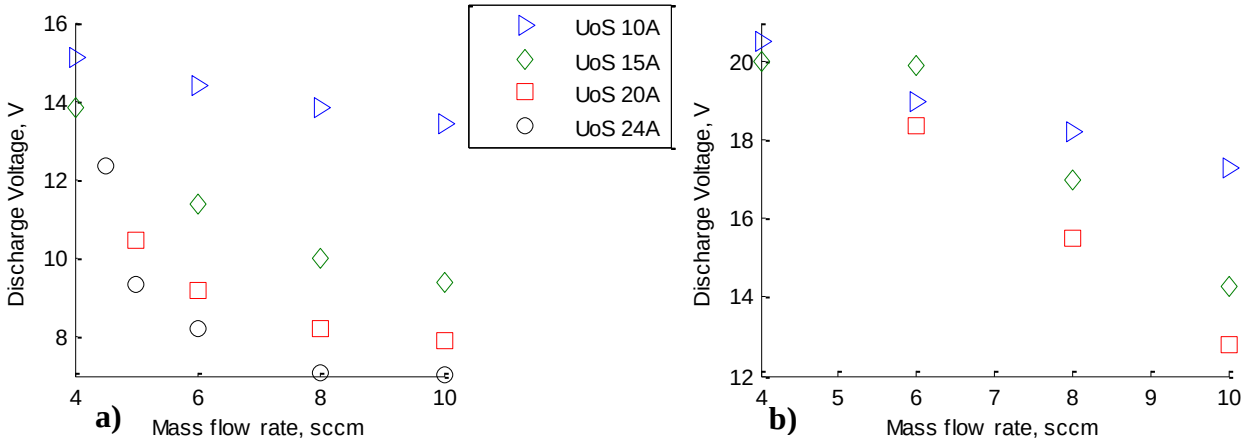

Figure 16. Discharge voltage for the T6 HCT a) without and b) with the magnetic field

As it can be seen as expected the discharge voltage decreases with increasing mass flow rates and discharge current. It can be noted how the discharge voltage increase due to the application of the magnetic field seems to depend mainly on the mass flow rate level with discharge voltage increasing abut 6V at 4sccm and 5V at 10 sccm regardless of the current level.

B. Cold gas T6 HCT thrust measurement at the UoS

Cold gas thrust measurements have been carried out at UoS for the T6 HCT. As expected Isp of about 20 seconds have been obtained.

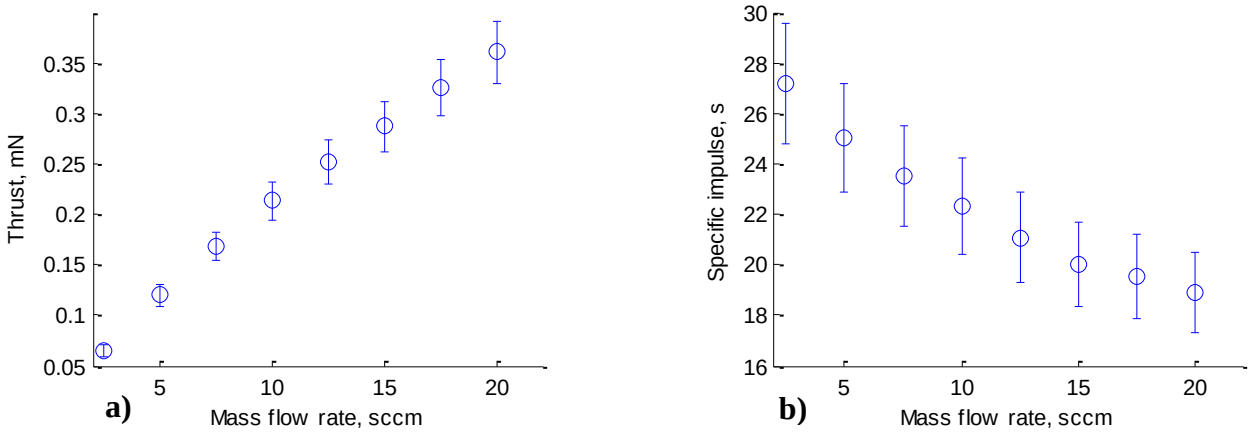

Figure 17. a) Thrust and b) specific impulse for cold gas on the T6 HCT

C. Discharge modes for T6 HCTs at the UoS and AER

Thrust measurements in the discharge mode were carried out on the T6 HCT at both UoS and AER and are reported below together with the predictions obtained with the theoretical model[7]. As it can be seen from the figures below the thrust trend with mass flow rate is almost linear with the specific impulse that decreases of about 40s when moving from 4 to 10 sccm.

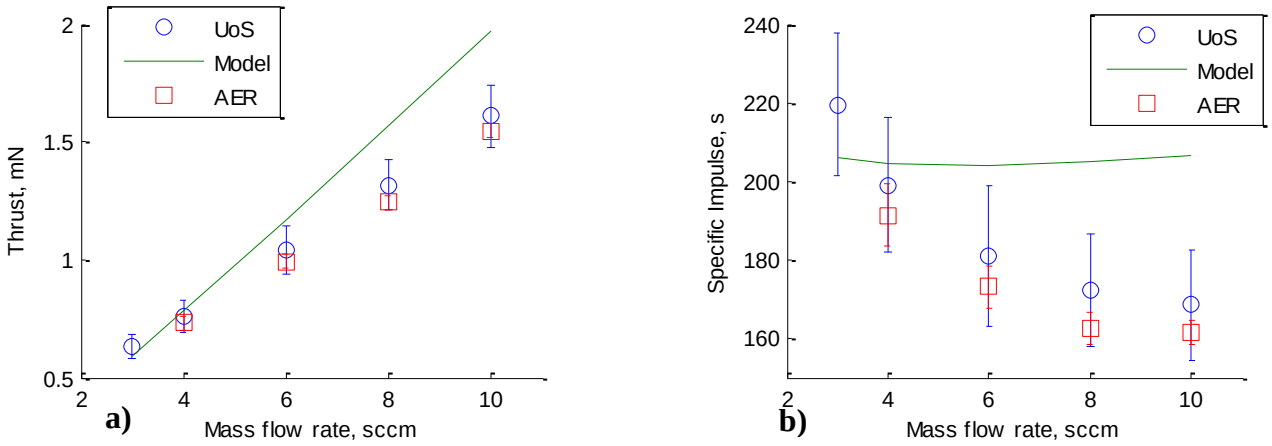

Figure 18. a) Thrust and b) specific impulse for T6HCT at 10A and comparison with model

The thrust range at 10 A of discharge current is 0.6 to 1.6 mN with the specific impulse ranging 220 to 170 s. The theoretical model provides values that show a maximum error on thrust of 18% at 10 sccm. It should be noted that the measurements performed with the two different direct thrust balances are in acceptable agreement with each other.

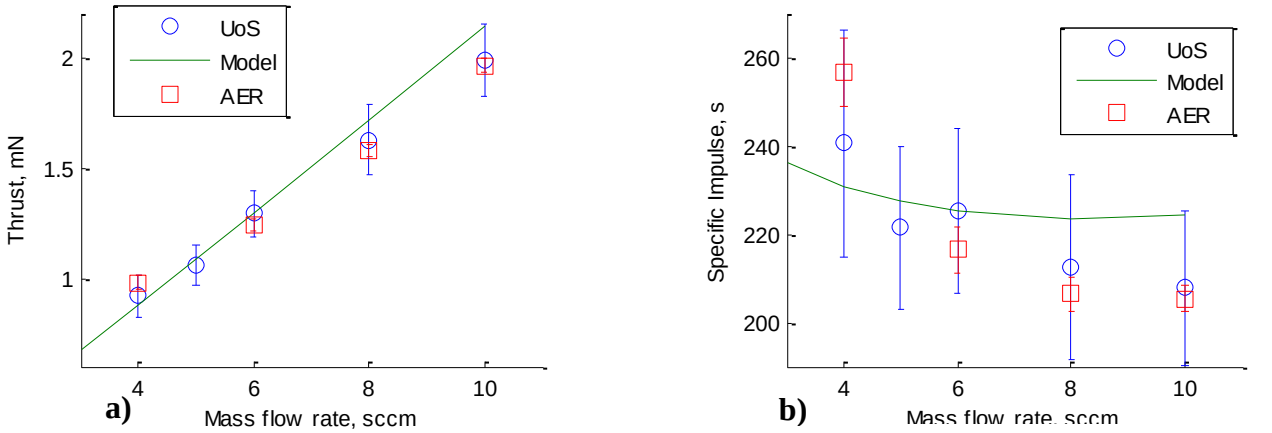

Figure 19. a) Thrust and b) specific impulse for T6HCT at 15A and comparison with model

The thrust range at 15 A of discharge current is 0.9 to 2 mN with the specific impulse ranging 240 to 210 s. In this case the agreement between the calculated and measured data is good showing a maximum error of 7% at 10 sccm that is within the UOS measurement error bars. It should be noted that also in this case the measurements performed with the two different direct thrust balances are in agreement with each other.

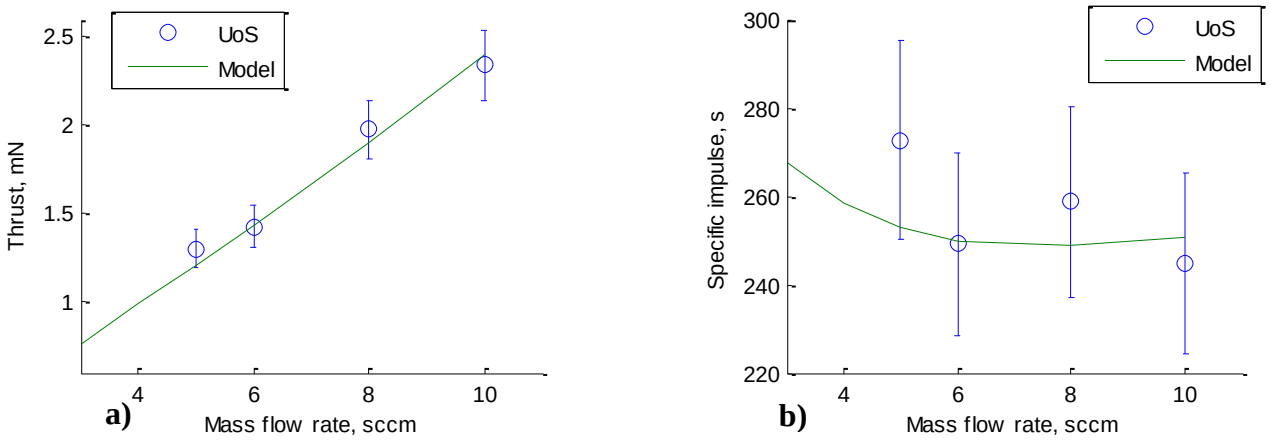

Figure 20. a) Thrust and b) specific impulse for T6HCT at 20A and comparison with model

The thrust range at 20 A of discharge current is 1.3 to 2.3 mN with the specific impulse ranging 273 to 244 s. Also in this case the agreement between the model and the measurement is good with a maximum error of 7% at 4 sccm. Since the thrust measurements carried out with the two thrust balances at 10 and 15 A were in good agreement with each other, it can be expected that the thrust measurements made at UoS at 20 A are reliable.

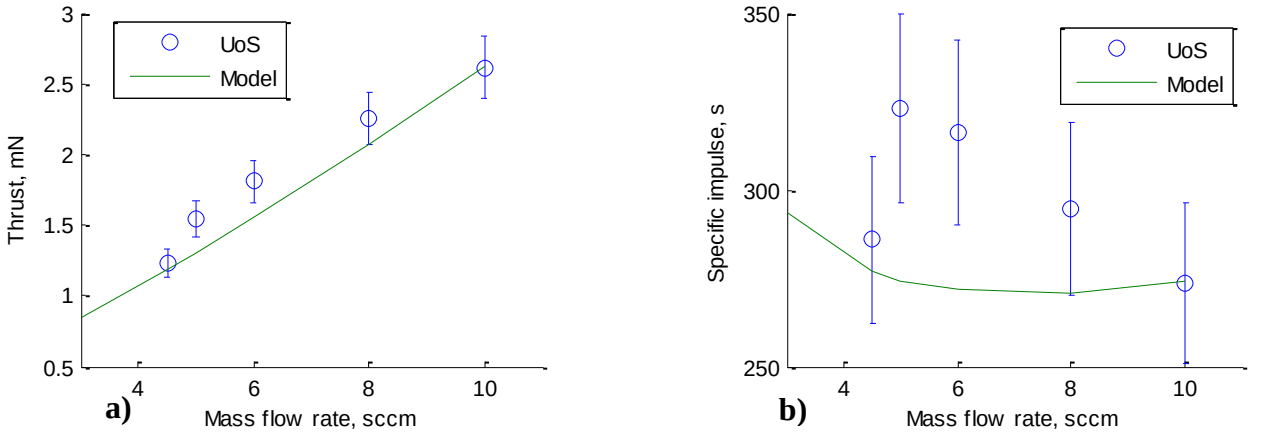

Figure 21. a) Thrust and b) specific impulse for T6HCT at 24A and comparison with model

The thrust range at 24 A of discharge current is 1.2 to 2.6 mN with the specific impulse ranging 325 to 275 s. The model agreement with the data is not as good as for the 15 and 20A case with a maximum error on the thrust of 17% at 5 sccm. These thrust measurements can also be considered acceptable as discussed for those at 20 A.
If we now compare the measured data with the requirements we can see how the thrust and *Isp* requirements can be both met at 24 A in the mass flow range going from 5 to 8 sccm of Xenon.

In Figure 22 to Figure 24 the thrust measurements performed with applied magnetic field are reported.

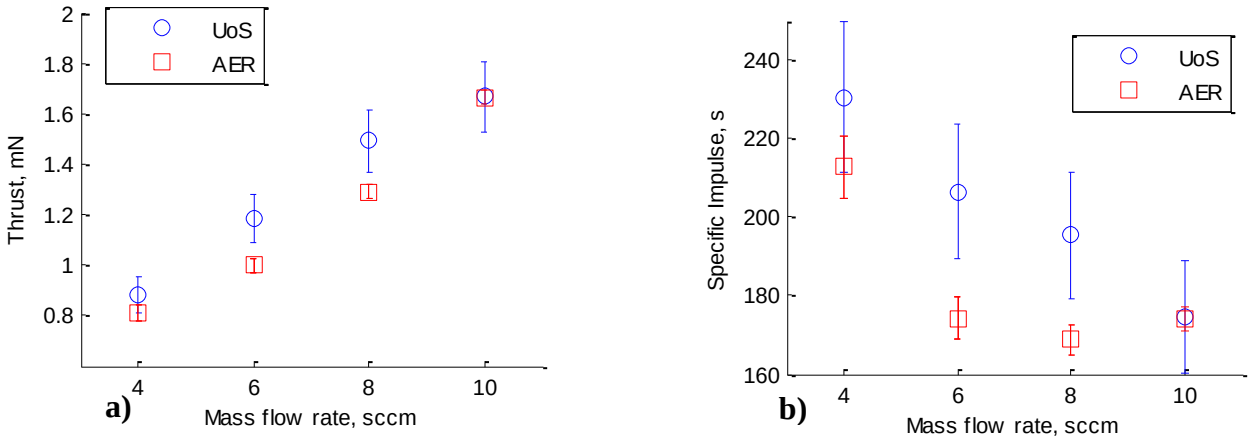

Figure 22. a) Thrust and b) specific impulse for T6HCT at 10A with the magnetic field

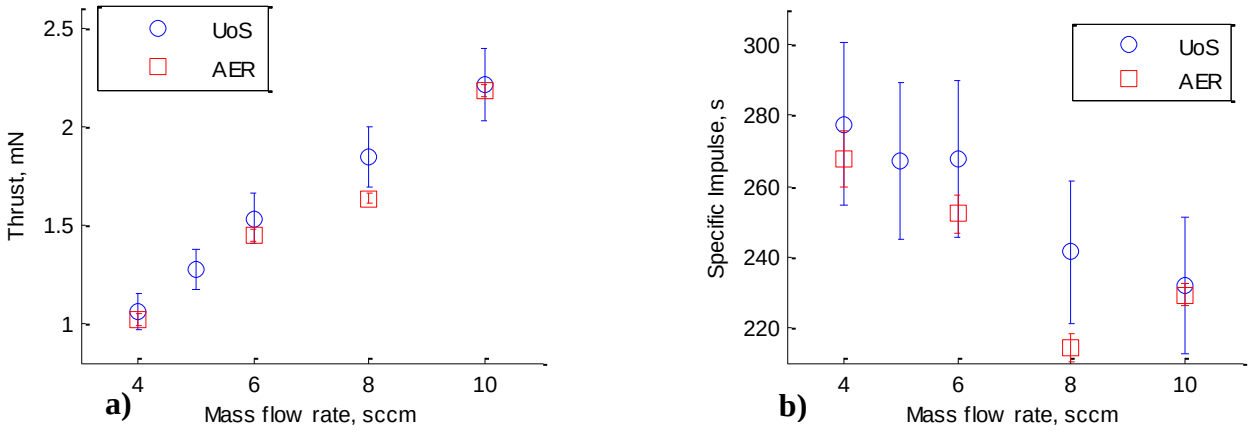

Figure 23. a) Thrust and b) specific impulse for T6HCT at 15A with the magnetic field

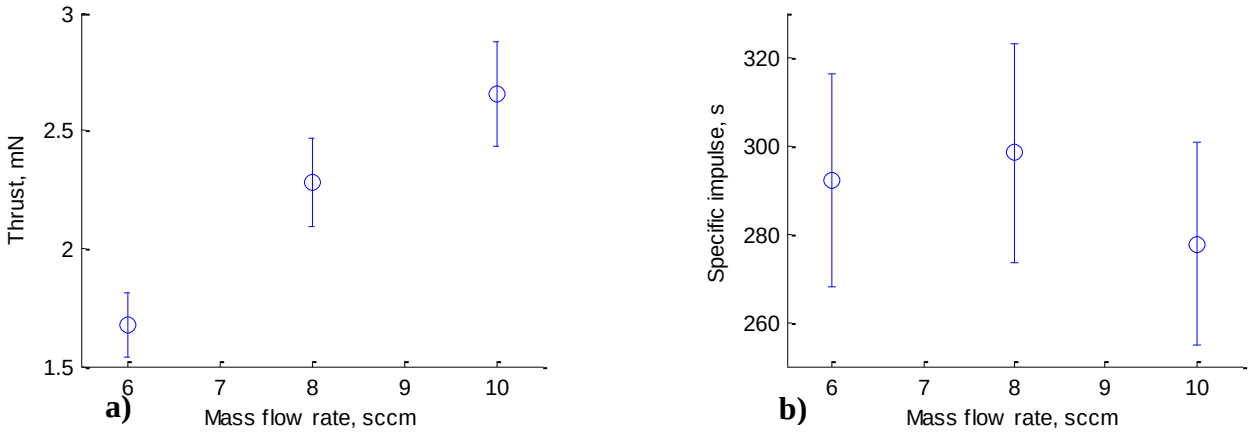

Figure 24. a) Thrust and b) specific impulse for T6HCT at 20A with the magnetic field

The thrust with applied magnetic field show a trend with mass flow rate that is qualitatively the same as the one seen without applied magnetic field with the thrust increasing almost linearly with increasing mass flow rates. Nevertheless the thrust values with applied field are higher than those without. For example an applied field of 86G produces an

increase of 0.12 and 0.2 mN respectively at 4 and 8 sccm at 10A of discharge current and a 0.24 mN increase at 20A and 6 sccm.
Comparing the applied field performance with the requirements shown in Table 1 it can be seen how the requirements are met at 20 A of discharge current and 8 sccm of Xenon.

In Figure 25 and Figure 26 all the data obtained with and without magnetic field are reported as a function of the propellant mass flow rate. In Figure 27 and Figure 28 the same data are reported as a function of the discharge current whereas in Figure 29 a comparison between the data with and without magnetic field in presented.

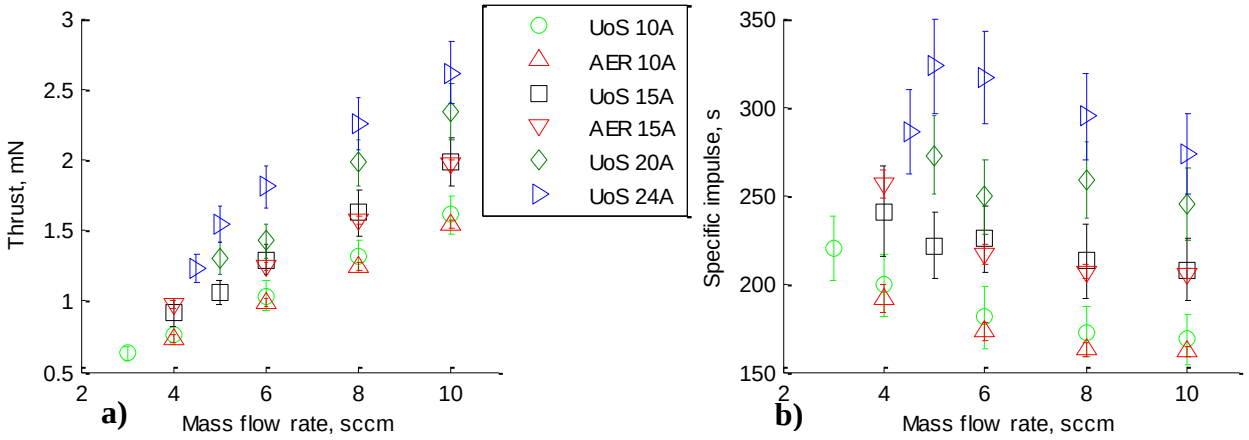

Figure 25. a) Thrust and b) specific impulse for T6HCT without magnetic field

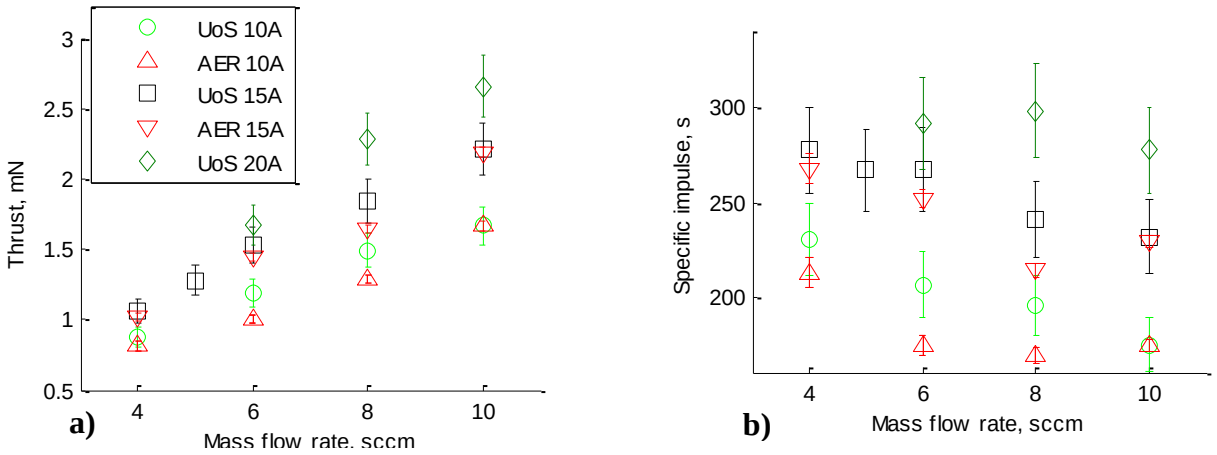

Figure 26. a) Thrust and b) specific impulse for T6HCT with the magnetic field

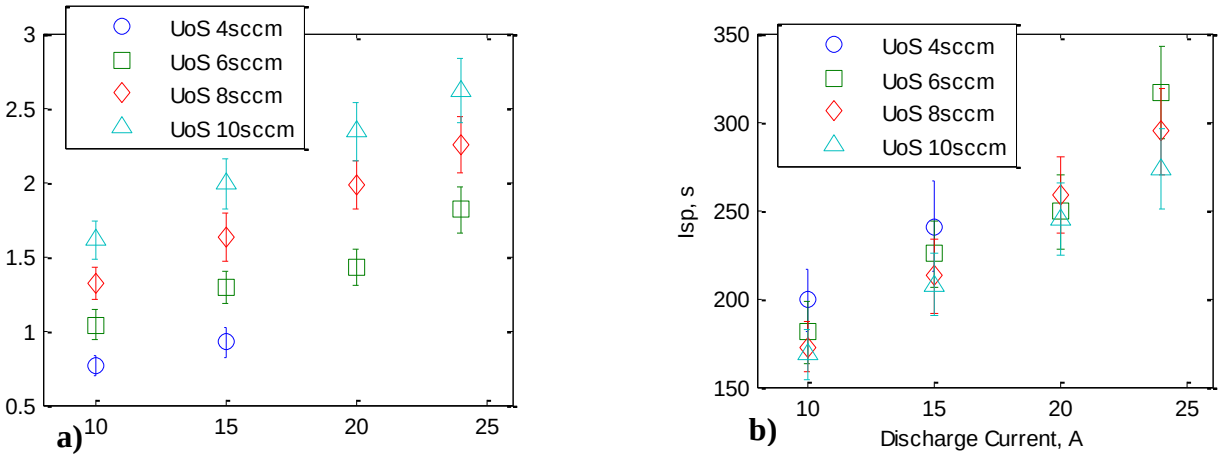

Figure 27. a) Thrust and b) specific impulse for T6HCT without magnetic field

As shown in Figure 27, both the thrust and the specific impulse increase linearly with the discharge current when the magnetic field is not applied.

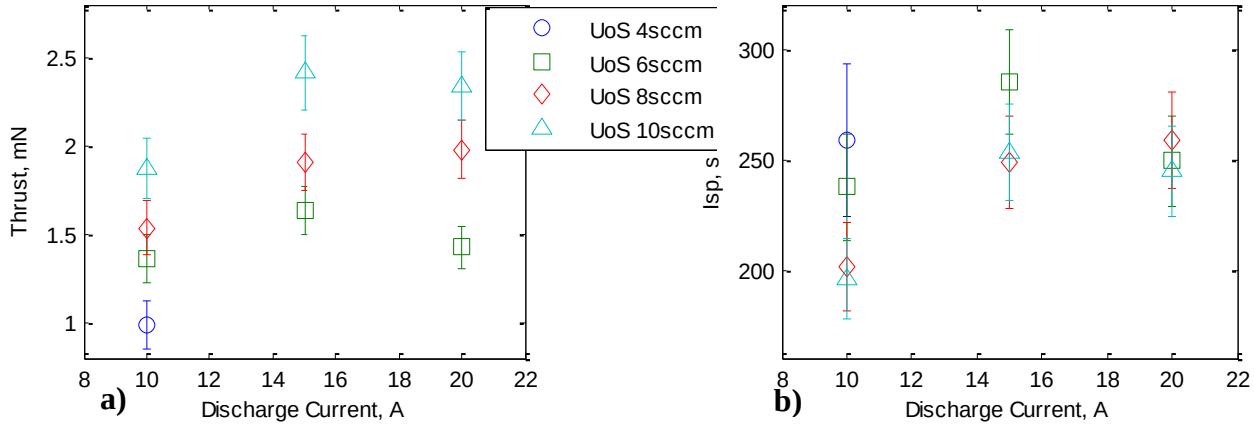

Figure 28. a) Thrust and b) specific impulse for T6HCT with the magnetic field

The thrust and the specific impulse seem to show a maximum at 15A of discharge current when the magnetic field is applied. The reason why this happens is not still completely understood and will be studied further in the future.

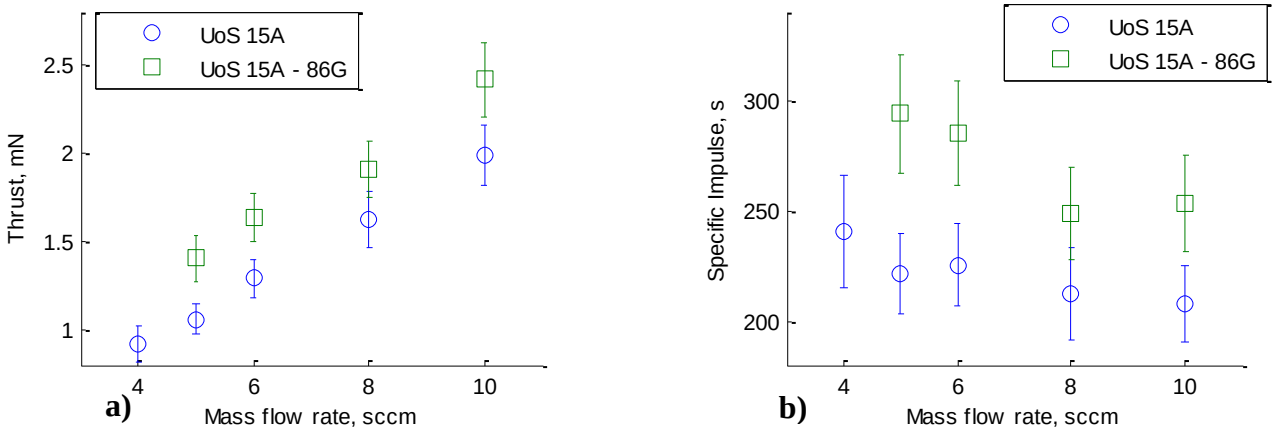

Figure 29. a) Thrust and b) specific impulse for T6HCT at 15A with and without the magnetic field

From Figure 29 it can be seen how the increase of the thrust due to the magnetic is a constant regardless the mass flow rate. From the data presented above the thruster propulsive efficiency can be derived as

$$\eta = \frac{T^2}{2\dot{m}(VI + P_m)} \quad (6)$$

where V and I are respectively the discharge voltage and current and P_m is the power needed by the coil.

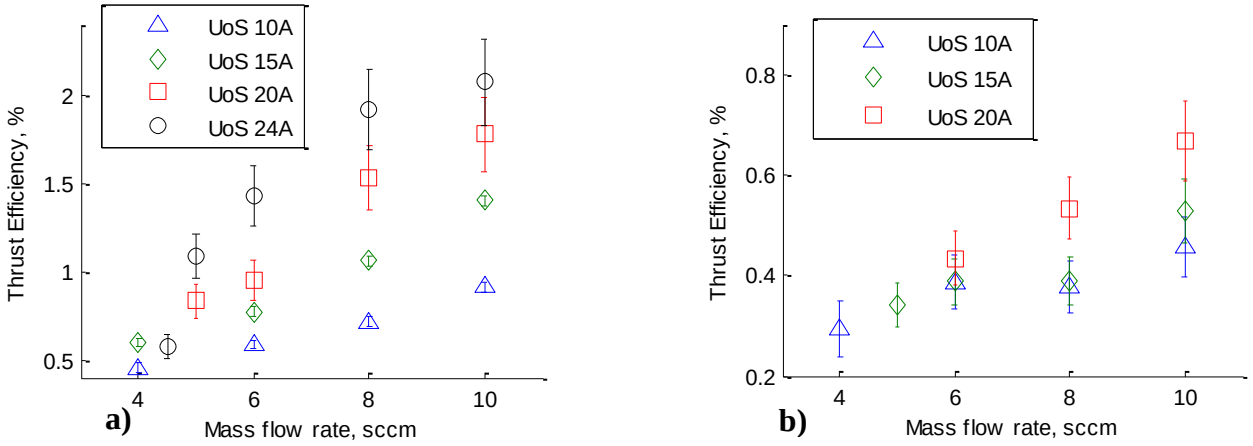

Figure 30. Thrust efficiency fir the T6 HCT a) without and b) with the magnetic field

As it can be seen from the figures above the efficiency increases with the mass flow rate and the discharge current, going up to 2.1% at 24A and 10 sccm with no magnetic field. It must also be noted that the use of the magnetic field significantly decreases the thrust efficiency.

VI. Optimized set-point

The requirements shown in Table 1 can be fulfilled at different conditions depending on the magnetic field. In Table 5 two different set-points with the T6 HCT are shown with the relative performances.

Parameters	T6 HCT No magnetic field	T6 HCT 86 G of magnetic field
Trust, mN	1.54 – 1.81 – 2.26	2.5
Isp, s	323 – 316 - 300	327
Mass Flow Rate, sccm	5 – 6 - 8	8
Discharge Current, A	24	20
Discharge Voltage, V	9.4 – 8.2 – 7.1	15.5
Efficiency, %	1.1 – 1.4 – 1.9	1.3
Total Power, W	225 – 197 - 170	330

Table 5. Performances of the T6 HCT to fulfill the requirements

VII. Conclusions

In this paper the results obtained from the test of an optimized HCT based on a QinetiQ T6 neutralizer have been presented. The T6 HCT tested differs from the conventional T6 neutralize design mainly by the orifice dimensions, which now is 2.5 mm long with the last 1 mm chamfered at 45 degrees of semi-angle and has a 0.2 mm diameter.

The HCT was tested at UoS and AER with two different direct thrust balances. At UoS test were carried out in cold gas mode measuring thrusts in the range 0.05 to 0.4 mN for mass flow rates of 2 to 20 sccm of Xenon with the specific impulse in the range 28 to 20 s.

The T6 HCT was tested in discharge mode both UoS and AER with and without an applied magnetic field of 86 G. The thrust was found to scale almost linearly with mass flow rate and with the discharge current. Maximum performances of 2.6 mN and 270 s were obtained at 24A of discharge current and 10 sccm of Xe. The application of a magnetic field was found to produce an increase in performance in terms of thrust and specific impulse but a significant decrease in terms of thrust efficiency mainly due to the increase in discharge voltage.

From the data obtained during the test campaign optimized set-points able to fulfill the requirements given in Table 1 of 300 s of specific impulse at 0.6 mN of thrust have been defined. In particular the requirements will be met at 24 A and 5, 6 or 8 sccm without applied magnetic field and at 20A and 8 sccm with the applied magnetic field.

Future works will focus on characterizing the performance increase due to the application of a magnetic field for various B field values. The theoretical HCT model will also be modified to include the effect relative to the application of a magnetic field.

References

[1]Gessini P., "Cathode Thrust Measurements Using a Target," PhD Thesis, University of Southampton, UK

[2]A.Grubisic. Microthrusters Based on the T5 and T6 Hollow Cathodes. PhD Thesis, UoS, Southampton, UK, 2009

[3]P. Gessini, S.B. Gabriel and D.G. Fearn - A Study of the Thrust Generated by a T6 Hollow Cathode, AIAA/ASME/SAE/ASEE 42nd Joint Propulsion Conference & Exhibit, AIAA Paper 2006-5265, 2006

[4]Gessini, P., Gabriel, S. B., and Fearn, D. G., "Hollow Cathode Thrust Measurements Using a Target: Initial Results and Some Issues," 28th International Electric Propulsion Conference, IEPC Paper 03-253, 2003

[5]A.N. Grubisic and S.B. Gabriel - Development of an indirect counterbalanced pendulum optical-lever thrust balance for micro- to millinewtons thrust measurement, Meas. Sci. Technol. 21 (2010)

[6]Grubisic A.N., Gabriel, S. B., and Fearn, D. G., - Preliminary Thrust Characterization of the T-Series Hollow Cathodes for All-Electric Spacecraft - IEPC-2007- 81

[7]D.Frollani, M.Coletti, S.B.Gabriel - A T5 Hollow Cathode Thruster: Experimental Results and Modelling – JPC 2012

[8]C.Edwards – Discharge Characteristics and Instabilities in the UK-25 Ion Thruster Operating on Inert Gas Propellants – PhD Thesis, University of Southampton

[9]Aston S.M.– Optical Read-Out Techniques for the Control of Test-masses in Gravitational Wave Observatories – PhD Thesis, University of Birmingham, 2011

[10]Riverhawk *Flexural pivot engineering data* http://www.flexpivots.com/

[11]Baker G.L, Blackburn J.A.– The Pendulum, A Case Study in Physics – Oxford University Press

[12] Taylor J R 1997 "An Introduction to Error Analysis. The Study of Uncertainties in Physical Measurements" 2nd ed (Mill Valley, CA: University Science Books)

[13]Ciaralli S Coletti M Gabriel S - An impulsive thrust balance for applications of micro-pulsed plasma thrusters, Measurement Science and Technology (accepted in August 2013, awaiting publication)